Transactions in GIS

WILEY

Transactions in GIS

RESEARCH ARTICLE OPEN ACCESS

Simulating Urban Economic Development in Metropolitan Areas Using Coupled S-Curve and Cellular Automata

Yao Yao[1,2,3,4,5] | Chenglong Zeng[2] | Jiayao Liu[2] | Dongsheng Chen[6] | Zhenhui Sun[7] | Kun Zhou[8] | Jiapeng Han[2] | Qingfeng Guan[2,3]

[1]Key Laboratory of Urban Land Resources Monitoring and Simulation, Ministry of Natural Resources, Shenzhen, China | [2]UrbanComp Lab, School of Geography and Information Engineering, China University of Geosciences, Wuhan, Hubei province, China | [3]National Engineering Research Center of Geographic Information System, China University of Geosciences, Wuhan, Hubei province, People's Republic of China | [4]LocationMind Institution, LocationMind Inc, Chiyoda, Tokyo, Japan | [5]Hitotsubashi Institute for Advanced Study, Hitotsubashi University, Kunitachi, Tokyo, Japan | [6]Chair of Cartography and Visual Analytics, Technical University of Munich, Munich, Germany | [7]Key Laboratory of Geographic Information Science (Ministry of Education), School of Geographic Sciences, East China Normal University, Shanghai, China | [8]Department of Architecture, National University of Singapore, Singapore, Singapore

Correspondence: Dongsheng Chen (dongsheng.chen@tum.de)

Received: 16 November 2025 | **Revised:** 6 August 2026 | **Accepted:** 27 August 2026

Keywords: cellular automata | continuous-state simulation | S-curve | spatiotemporal modeling | urban economic forecasting

ABSTRACT

Urban economic forecasting is crucial for the formulation of a macroeconomic development strategy for a region toward harmonious socio-economic and ecological progress. Cellular Automata (CA) enables fine-grained urban economic modeling, but its conventional discrete-state structure performs poorly when handling continuous economic variables like GDP density, and furthermore often lacks the ability to integrate with general economic growth patterns. These shortcomings ultimately compromise the simulation accuracy of urban economic dynamics. This paper innovatively proposes a continuous-state Density Cellular Automata (DCA) framework integrated with S-shaped economic growth responses, aiming to enhance GDP density simulation accuracy. Taking the Wuhan metropolitan area as a case, we simulated the 2010–2020 GDP density evolution and compared the performance with two baseline models. The results indicate that all cities in the metropolitan area follow S-shaped growth but with significant inter-city differences. The DCA demonstrates a 58.21% reduction in MAE compared to the discrete-state PLUS model and a 29.78% decrease in RMSE relative to the conventional continuous-state Gray-Cells CA model. The scale effect analysis shows that smaller zoning scales improve the accuracy of economic simulations. DCA can provide references of economic trends and support urban planners and managers in balancing urbanization with the ecological environment.

1 | Introduction

The rapid economic growth has precipitated a multitude of environmental challenges, including notable increases in environmental pollution (J. Liu and Diamond 2005), resource overconsumption (Z. Liu, Guan, et al. 2015; Liu, Luo, et al. 2015), ecological degradation (Luo and He 2023), and health issues (X. J. Yang 2013), etc. These issues hinder the sustainable development of cities, as urban economic development strategies frequently exert undue influence over city development policies in many countries (Dahiya 2014). Over the past decades, urban GDP growth has had a positive impact on urban land expansion (Mahtta et al. 2022). The metropolitan area is an essential subject of urban economy. In the process of economic development and urbanization, the boundaries between neighboring cities continue to expand and gradually merge into a multi-city, interdependent metropolitan area (Chuanglin Fang and Yu 2017). The metropolitan areas are defined as regions with a significant concentration of resources, including population, capital, technology, and innovation. Economic integration optimizes resource allocation and improves land use efficiency (X. Gao et al. 2020). Therefore, the analysis of economic development in metropolitan areas is crucial in the study of sustainable urbanization and ecosystem coordination.

Recently, Cellular Automata (CA) has been adopted as an innovative way for urban economic simulation to provide fine-grained spatial information for economic geographers and urban planners (Tu et al. 2024; Yao et al. 2023; Zeng et al. 2025). The conventional methods of urban economic forecasting often prove inadequate in generating results that incorporate sufficient spatial information, such as linear regression (Peters 2001), time series forecasting (Sezer et al. 2020), and causal analysis methods (Baker et al. 2015). These approaches typically assume uniform economic behavior across space, neglecting intra-city heterogeneity in density, resource distribution, and agglomeration effects. Furthermore, traditional models struggle to capture nonlinear growth patterns, threshold effects, and spatial spillovers that characterize high-density urban environments. CA models compensate for the limitations of conventional economic forecasting models by focusing on the local interactions of cells with coupled characteristics in discretized times and spaces. The state-of-the-art CA models for the purpose of urban economic forecasting are principally concerned with the relationship between land use changes and economic dynamics (Tu et al. 2024; Yao et al. 2023). The model provides insights into the underlying mechanisms of urban economies by capturing how shifts in land use, such as regional urban expansion or changes, influence economic activities like investment and job creation. The establishment of this connection facilitates precise predictions of the spatiotemporal changes of urban economies, thereby ensuring sufficient spatial information for effective metropolitan planning (Yao et al. 2023).

However, conventional urban CA models are designed to model urban land in discrete states (X. Liu et al. 2018; Y. Liu et al. 2021). They can result in biases in urban economic forecasting as they typically discretize regional economy into discrete levels (Figure 1A). Some scholars have attempted to integrate the densification process of urban density into CA, such as the logistic regression-based CA model (Mustafa et al. 2018). However, it still classifies urban building density into three discrete categories (low, medium, and high), which can only provide limited reference for urban planning.

Representing urban land with continuous states in CA models, as opposed to discrete states, has the potential for better economic forecasting (Chakraborty et al. 2022). A representative model is the gray-cells CA model (Yeh and Li 2002), which proposed the concept of urban density to represent the continuous states of urban land. Urban density has two-fold meanings, as shown in Figure 1B. It refers to the urban development density within a cell when it ranges from 0.0 to 1.0. While it can represent continuous variables of interest (e.g., economic density and population density) once it accumulates to more than 1.0. Considering the impact of urban density in the simulation of urban development helps to better understand the urban development trends as urban density is crucial in the process of urban development (Yeh and Li 2002). However, the gray-cells CA fails to capture the complex urban density distribution of metropolitan areas as the model is built based on the urban-center distance decay model (Clarke and Gaydos 1998). It assumes a negative exponential decay of urban density as the distance from the city center increases. This geographic-determinism assumption is applicable only to an ideal city with a concentric zone spatial structure. However, urban development has a spatially heterogeneous nature and is affected by the interactions among diverse land uses. Consequently, the model may only be applied to scenarios that meet the strong assumption, providing a limited reference for complex and diverse urban planning scenarios (K. Gao et al. 2021).

The S-curve-based CA model for urban economic forecasting provides the potential of a shift from the geographic-determinism assumption to the paradigm of evolutionary spatiotemporal dynamics (Siedlecki et al. 2018). Unlike alternative nonlinear forms such as power functions that lack growth saturation or regression approaches such as logistic regression that focus on binary state transitions, the S-curve inherently captures both the initial acceleration and later saturation of GDP growth. These two characteristics are key features of metropolitan economic development, which is constrained by resources and infrastructure. The growth of the economy universally exhibits an S-curve trend, characterized by the experience of faster growth rates followed by lower growth rates due to resource constraints and finally slowing down and converging to zero (Yao et al. 2023). The S-curve model reflects a trajectory of steady and gradual advancement in economic development (Sng 2010). Thus, it is commonly employed in urban economic studies, such as those investigating the relationship between energy demand and GDP per capita (Wang et al. 2015), the composition of exported goods and GDP (Hu et al. 2012), and the prediction of spatiotemporal trends in urban economic development (Yao et al. 2023). Later, the S-curve model was employed in the analysis of urbanization, representing the expansion of urban density in the vertical spatial direction (Jinqiang He, Wang, et al. 2017; Jiao 2015; X. Liu et al. 2018). The S-curve models urban continuous variables from a time dimension without relying on spatial dimension assumptions in urban spatial models. Thus, it can depict the spatial unevenness of urban development and aid in modeling urban economy in metropolitan areas from a perspective of regional temporal trends (Cao et al. 2020).

This study proposes the Density Cellular Automata (DCA) framework for urban economic simulation and forecasting based on the CA model and S-curve model (Figure 1C). The framework is based on a continuous state-based CA model for simulating continuous urban density. Meanwhile, the framework divides the metropolitan area into multiple regions. The S-curve model is introduced to better simulate the trend of economic growth of the metropolitan area. The DCA aims to expose the complex economic distribution in the metropolitan area with sufficient spatial information. The result generated by the proposed framework can provide references and insights for metropolitan development planning.

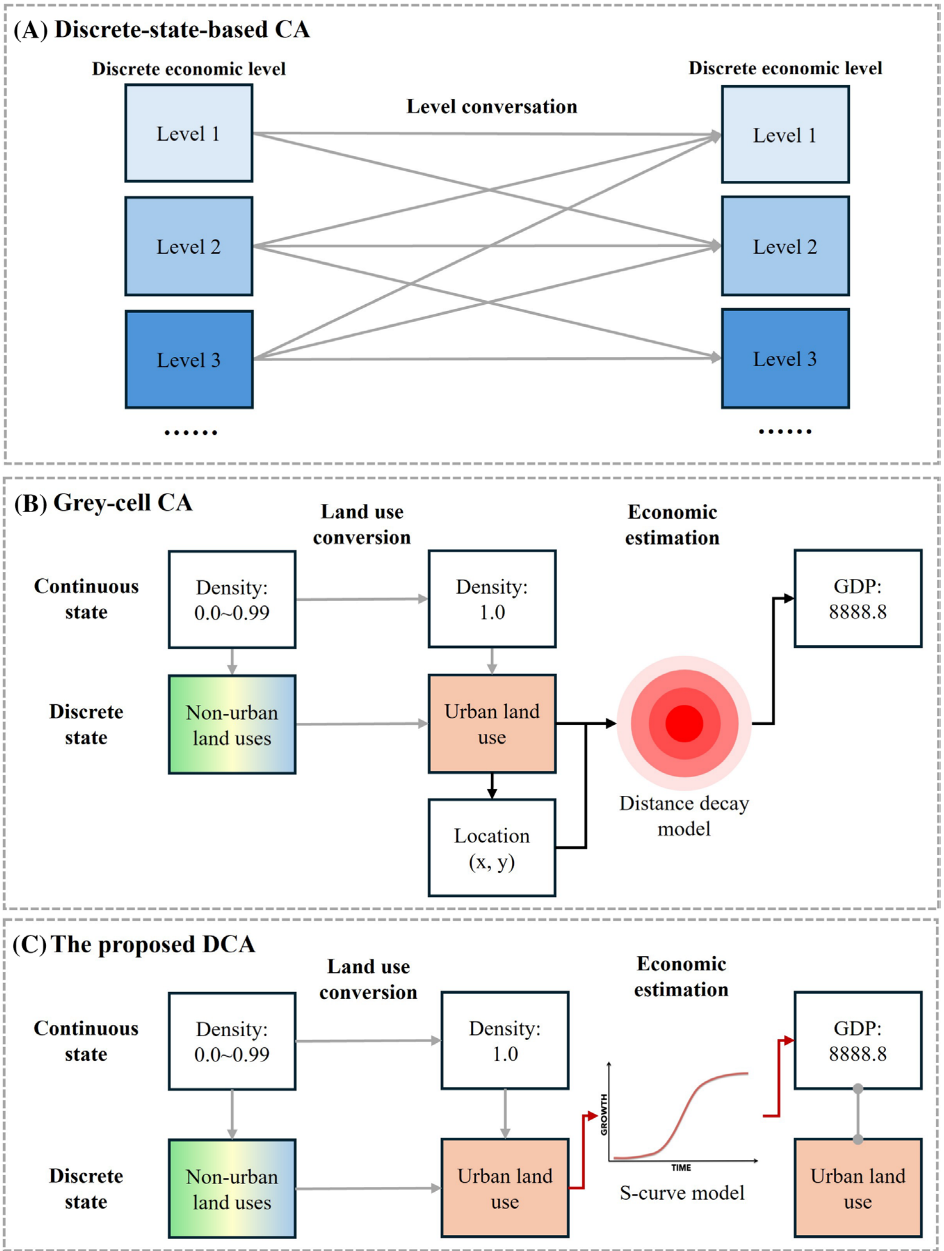

FIGURE 1 | Differences in key mechanisms among different CA models for spatial economic simulation. (A) Conventional discrete-state based CA. (B) Gray-cell CA, a representative continuous-based CA model. (C) The proposed DCA.

2 | Study Area and Data

The Wuhan "1 + 8" metropolitan area is taken as the study area. The term "1 + 8" refers to the metropolitan area encompassing eight neighboring large and medium-sized cities, with Wuhan, the largest city in central China, serving as the central city. The study area constitutes one-third of the Hubei Province's total land area and one-half of its population (https://www.hubei.gov.cn/). It's characterized by the most intensive economic development and the most substantial economic strength in the province. Metropolitan areas have become essential pivotal drivers of economic, industrial, and technological innovation after the reform and opening up of China (Tian 2020). Nonetheless, the Wuhan metropolitan area exhibits a more pronounced urban–rural dual economic structure in comparison to other metropolitan areas (Y. Liu, Guan, et al. 2015; Liu, Luo, et al. 2015). This is evidenced by the concentration of modern industries in urban areas and the predominance of traditional agriculture in rural areas (Ke et al. 2021). This inherent complexity renders the Wuhan metropolitan area a challenging case region for this study.

Three types of data are primarily utilized, including land use data, GDP distribution data, and spatial auxiliary variables. In particular, the land use data are derived from China's 30-m annual land use data for 2010 and 2020 produced by the Center for Resource and Environmental Science and Data Platform of the Chinese Academy of Sciences (https://www.resdc.cn/). The data categorizes six types of land use (Figure 2), including crop land, forest land, grass land, water, building land,

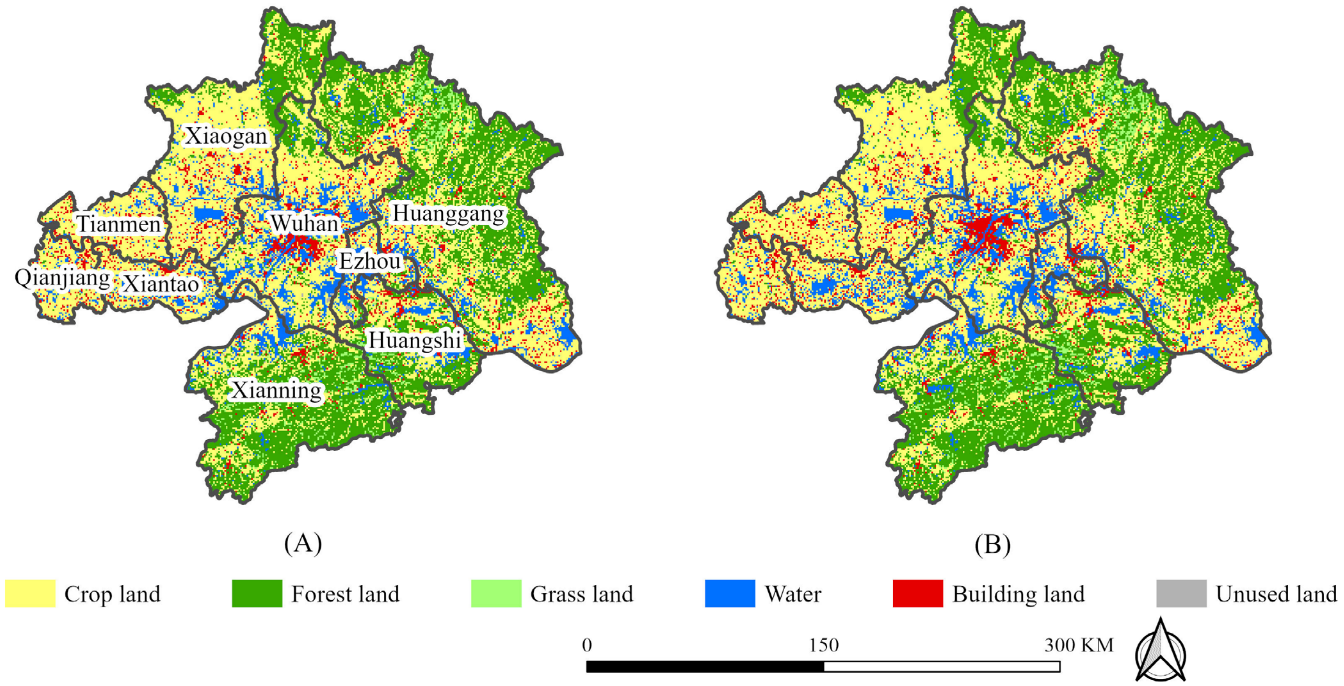

FIGURE 2 | Urban land use data for Wuhan metropolitan area in (A) 2010 and (B) 2020.

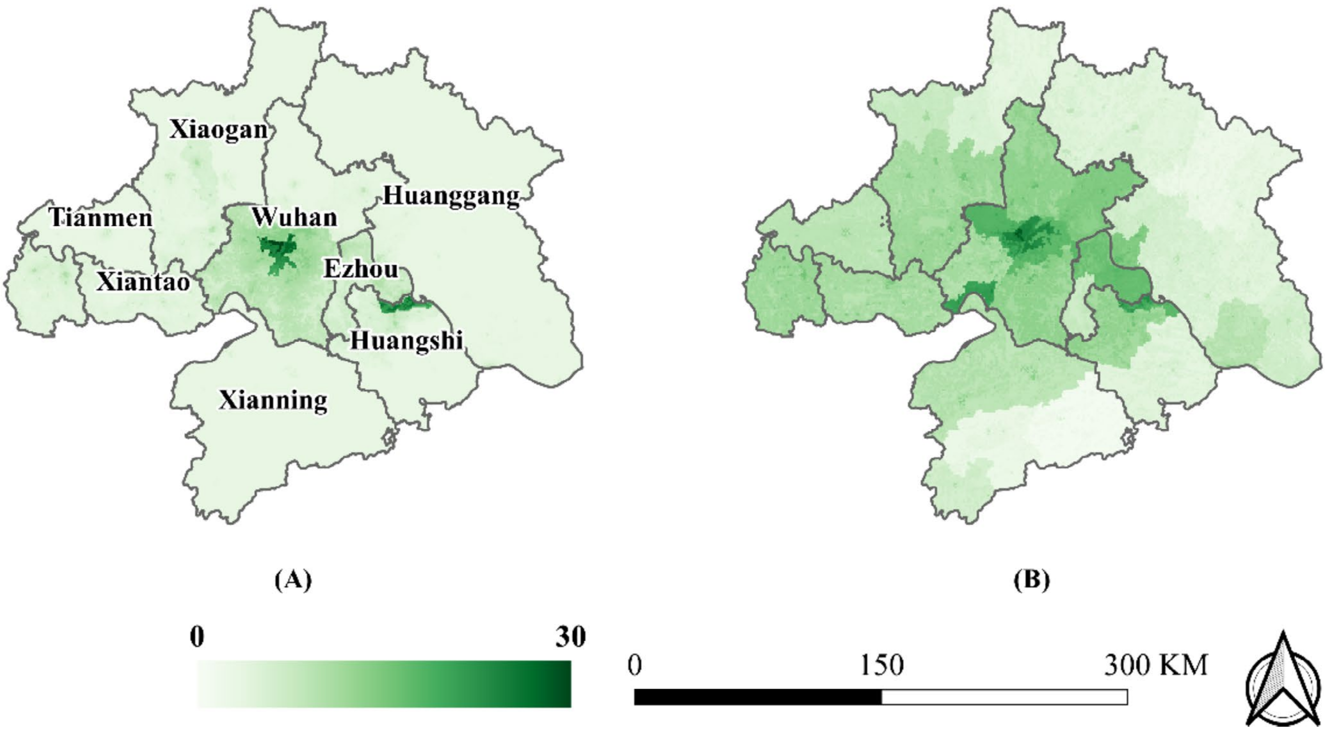

FIGURE 3 | GDP distributions (10,000 CNY per km^2) in Wuhan metropolitan area in (A) 2010 and (B) 2020.

and unused land, which can be divided into urban and non-urban land use. The GDP distribution data show the spatial distribution of China's GDP in 2010 and 2020 on a kilometer grid, which are also obtained from https://www.resdc.cn/. To ensure the alignment of the data sets at the same scale, a re-sampling pre-processing was employed to match the resolutions of both the land use data and the GDP data, resulting in a 1 × 1 km grid (Figure 3).

We also applied Gaode's Point-Of-Interest (POI) data (https://lbs.amap.com/), Open Street Map (OSM) data (https://www.openstreetmap.org/), and DEM data to construct spatial auxiliary variables jointly, representing topographic, industrial, commercial, and other drivers affecting GDP and land use change. DEM data were reconstructed from remote sensing imagery (Yuan et al. 2023), and data tiles were mosaicked to cover the entire study area (Yuan et al. 2024). Subsequently, the slope

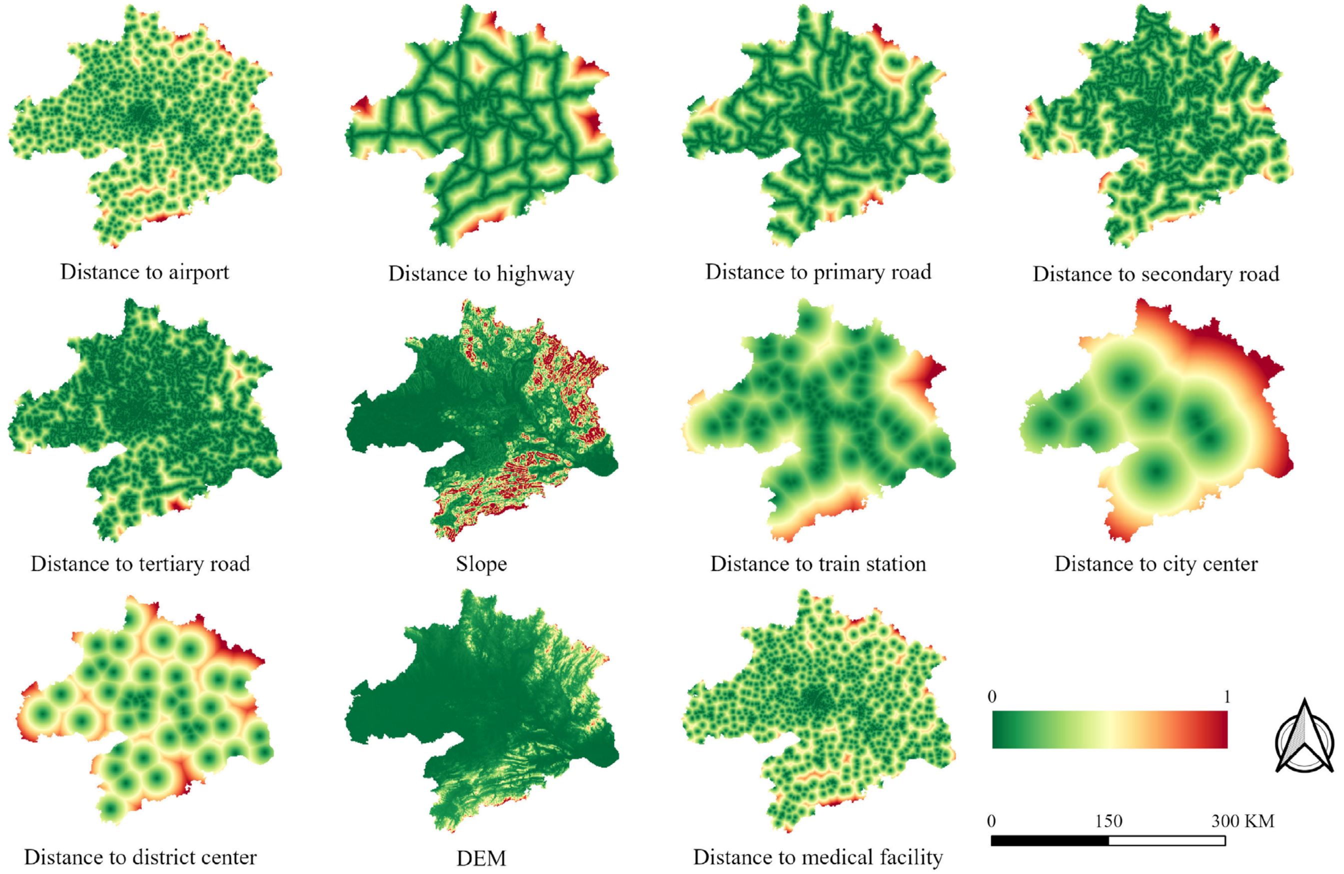

FIGURE 4 | Spatial auxiliary variables constructed in this study.

variables were calculated based on DEM data. The spatial resolutions of spatial auxiliary variables were set to 1×1 km, and all the variables were normalized to [0, 1] (Figure 4).

3 | Methodology

Figure 5 illustrates the workflow of the proposed DCA model, consisting of three steps. (1) Construction of DCA—this step aims to construct a continuous state-based CA model by incorporating the state and initial density of the cells with the concept of "gray cells" to represent continuous state changes. (2) Construction of S-curve models—this step involves the construction of S-curve models to fit the trends of GDP growth for various geographical regions. (3) Urban economic simulation—the purpose of this step is to simulate the urban GDP growth using fitted S-curve models and cellular conversion rules.

3.1 | Construction of Density Cellular Automata Model

In existing research of CA-based urban land use simulation, the conversion rules of CA models determine the conversion of cell states. Existing research has identified that population growth and related urban density drive changes in urban land use (J. Yang et al. 2023). This study proposed to integrate cell density of development into the previous cell state-based conversion rules. Thus, the conversion rules for continuous data are jointly determined by the cell state and cell density of development:

$$\left(S^{t+1}, \text{Density}^{t+1}\right) = f\left(S^t, \text{Density}^t, N\right) \tag{1}$$

where $S^t, \text{Density}^t, N$ indicate the cell state, the cell density at time t, and the impact of the neighboring cells within a neighborhood range. In this model, the concept "gray cells" refers to the continuous states of the cells ranging from 0 to 1. The attainment of a value of 1 by the continuous cell states signifies the conversion of the "gray cells" into urban land. The continuous cell state ΔG_i^t is determined by the cell density and the impact of neighboring cells and constraints:

$$\Delta G_i^t = f\left(\text{Density}_i, N\right) \times f_{\text{develop}}\left(\delta_i, N\right) \tag{2}$$

where $f\left(\text{Density}_i, N\right)$ refers to the effect of the cell densities within the N neighborhood range on the change of the continuous cell state. While $f_{\text{develop}}\left(\delta_i, N\right)$ is the development speed of the cells. This equation indicates that the higher the economic levels within the neighborhood range, the higher the corresponding urban density of development, the greater the possibility of converting the land use type, and the faster the change in the continuous cell state. Therefore, the change of the continuous cell state is formulated as follows:

The neighborhood impact function $f\left(\text{Density}_i, N\right)$ quantifies the influence of surrounding urban cells on the target cell, calculated as:

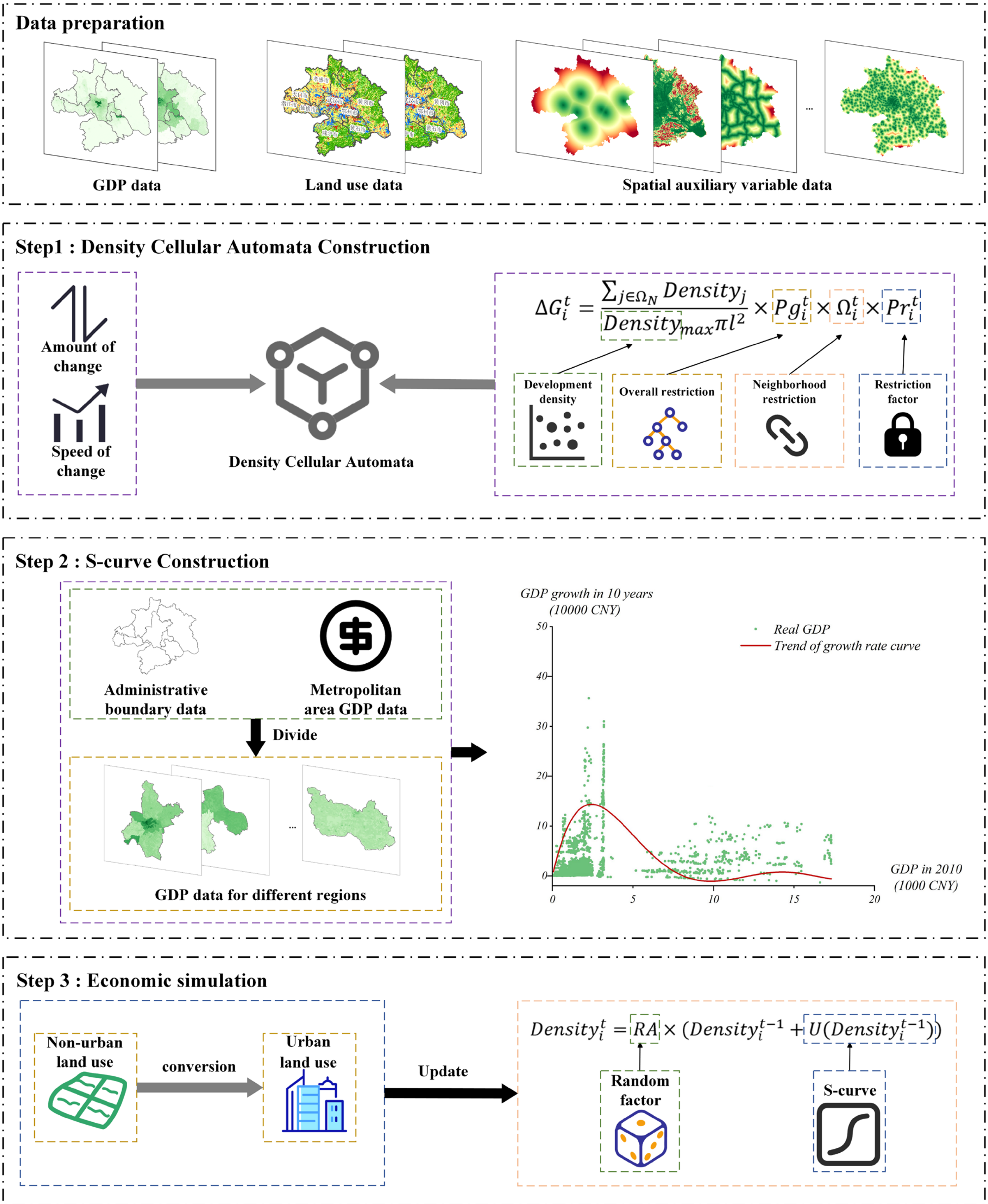

FIGURE 5 | Workflow of the proposed DCA framework.

$$f\left(\text{Density}_i, N\right) = \frac{\sum_{j\in\Omega_N} \text{Density}_j}{\text{Density}_{\max}\pi l^2} \tag{3}$$

where N denotes a Moore neighborhood, which includes 8 surrounding cells, to capture comprehensive spatial interactions. l is set to 1 km to align with the 1×1 km grid resolution of this study. Ω_N refers to the neighborhood effect of a set of cells that have been converted into urban land within the neighborhood range N. While Density_j indicates the cell density of the *j-th* urban land. $\text{Density}_{\max}$ refers to the maximum cell density of development within the Ω_N set.

The overall constraint function in the proposed DCA model includes the overall development probability Pg based on spatial auxiliary driving factors, the neighborhood development constraint function Ω, and the limiting factor Pr. The difference function of the continuous cell state is formulated as follows:

$$\Delta G_i^t = \frac{\sum_{j \in \Omega_N} \text{Density}_j}{\text{Density}_{\max} \pi l^2} \times Pg_i^t \times \Omega_i^t \times Pr_i^t \tag{4}$$

where Pg_i^t is calculated via the relationship between the spatial auxiliary variables X and the converted type of land use Y. A $Y = f(X)$ model was constructed, and the probability of the land use type of the cell converting into the *i-th* type Y_i was determined to be the overall development probabilityPg_i^t.

3.2 | Construction of S-Curve Models

In this study, it is found that the growth rate curve of GDP exhibits the characteristics of a derivative of an S-curve (see Section 4.1). Following an initial period of sluggish growth, the GDP demonstrates a dynamic growth rate until the growth rate attains its maximum value. Thereafter, the growth rate gradually decelerates until it attains a state of zero growth. Therefore, we construct an independent S-curve model for each administrative unit to simulate the regional economic growth. The S-curve model for GDP is formulated as follows:

$$U(\text{density}) = \frac{x_m}{1 + \left(\left(x_m / x_0 - 1 \times e^{-r * \text{density}} \right) \right)} \tag{5}$$

where density represents the initial urban development density input into the model. x_m represents the asymptotic maximum GDP density and represents the estimated long-term upper level of regional economic output under the historical development regime. While x_0 denotes the initial GDP density, and r is the intrinsic growth-rate parameter controlling how rapidly GDP density approaches x_m. The parameters x_m, x_0, and r were estimated separately for each administrative unit using nonlinear least squares and historical GDP-density observations. Thus, they are assumed to remain constant over the simulation period.

3.3 | Urban Economic Simulation

In the majority of conventional CA models, the change of cell state from 0 to 1 indicates the conversion of land use type in the cell. However, in the proposed DCA model, the change of cell state not only determines the conversion of land use type but also determines the change of cell density of urban development. Given any timestamp, the continuous cell state can be obtained via the below equation:

$$G_i^{t+1} = G_i^t + \Delta G_i^t \tag{6}$$

A metropolitan region is an open complex urban system whose economic growth is influenced by multiple factors, which are unpredictable. It is a common practice in CA models to incorporate these unpredictable effects as a significant component of simulation systems (Hoshovska et al. 2020). Here, DCA also introduces a random variable to represent the unpredictable effects on economic growth in the context of open complex urban systems. The equation for the random variable is as follows:

$$RA = 1 + \frac{\gamma - 0.5}{0.5} \times \beta \tag{7}$$

where γ is a random number evenly distributed in the range [0,1], and β is a fractional multiplier that controls the size of the random variable. Mathematically, since $\frac{\gamma - 0.5}{0.5}$ ranges from −1 to 1, RA spans $1 - \beta$ to $1 + \beta$. Compared with population density, GDP density exhibits stronger short-term spatial volatility due to firm entry and exit, industrial restructuring, and project-based economic activities. Therefore, a relatively larger stochastic fluctuation range controlled by β is required to represent uncertainties in economic dynamics. Here, β regulates the amplitude of the random allocation term RA without changing the expected density trajectory, while the deterministic economic evolution is mainly governed by the S-curve growth function and CA-based spatial transition mechanisms. The sensitivity analysis in Table S7 indicates that $\beta = 1$ achieves the best simulation performance, suggesting that this setting better captures the heterogeneous and dynamic characteristics of economic activities.

The S-curve-based overall density for urban economic simulation can be formulated as follows:

$$\text{Density}_i^t = \text{RA} \times \left(\text{Density}_i^{t-1} + U\left(\text{Density}_i^{t-1} \right) \right) \tag{8}$$

where $U(*)$ refers to the S-curve model constructed in this study.

3.4 | Baseline Models for Economic Simulation

Pixel-level economic simulation:

- Discrete-state CA: This study adopts the Patch-generating Land Use Simulation (PLUS) model (Liang et al. 2021) as a representative discrete-state CA model for comparative experiments. The PLUS model exemplifies advanced discrete-state CA systems by simulating land-use transitions through cell state changes while incorporating two key innovations. (1) A land expansion analysis strategy that overcomes the limitations of traditional CA in driver interpretation by quantifying transition rules via expansion patterns, as opposed to the exhaustive “from-to” combinations. And (2) a multi-type random patch seeding mechanism that enables organic patch evolution for diverse land-use classes. It addresses the typical deficiency of discrete-state CA in simulating fine-scale landscape dynamics. It maintains the core principles of conventional CA models, including local interactions, state discreteness, and spatiotemporal dynamism. Hence, PLUS is an ideal baseline for representing existing discrete-state CA models.
- Continuous-state CA: The Gray-cells CA model is adopted as a representative continuous-state CA model for comparative experiments. It introduces the concept of “gray cell,” representing the continuous level of urbanization. The model incorporates three core components, i.e., (1) a density decay function assigning location-specific development densities based on distance from urban centers, (2) the environmental and urban-form constraint functions regulating

development suitability, and (3) the stochastic variables introducing unpredictable density variability. This model provides a contrast to discrete-state approaches in evaluating density-sensitive urban dynamics.

City-level economic simulation:

- Autoregressive Integrated Moving Average (ARIMA) model: is a time series forecasting method based on the assumptions of linear structure and stationarity. Its model consists of three parts: autoregression, differencing, and moving average. ARIMA, with its ability to analyze linear trends in time series, is a classic statistical model for short-term forecasting of macroeconomic indicators (Abonazel and Abd-Elftah 2019).
- Random Forest (RF) model: is a nonlinear regression method based on decision tree ensemble that improves prediction robustness through Bootstrap aggregation and feature randomness. The RF model excels at capturing complex nonlinear relationships and is particularly effective in modeling financial market fluctuations and multivariate economic systems (Yoon 2021).

3.5 | Accuracy Assessment

The task of this study aims to simulate the spatial evolution of GDP, a continuous variable. The evaluation metrics for the conventional discrete-state CA models are not suitable for the task at hand. Consequently, the Mean Absolute Percentage Error (MAPE), Root Mean Square Error (RMSE), and Mean Absolute Error (MAE) are applied instead to evaluate the performance of urban economic development simulation.

MAPE, RMSE, and MAE are classic evaluation metrics for regression evaluation. MAPE appears in the form of a percentage, representing the average percentage of relative difference between predicted and actual values. RMSE calculates the square root of the sum of squares of differences between predicted and real values. While MAE indicates the absolute error between predicted and real values. The smaller the metrics are, the stronger the prediction ability of the model is. Among them, however, RMSE is greatly affected by the distribution bias. In contrast, MAE can better reflect the performance of models' average errors (Willmott and Matsuura 2005).

The equations of RMSE, MAPE, and MAE can be calculated as follows:

$$\mathrm{RMSE} = \sqrt{\frac{1}{n}\sum_{i=1}^{n}\left(\hat{y}_i - y_i\right)^2} \tag{9}$$

$$\mathrm{MAPE} = \frac{100\%}{n}\sum_{i=1}^{n}\left|\frac{\hat{y}_i - y_i}{y_i}\right| \tag{10}$$

$$\mathrm{MAE} = \frac{1}{n}\sum_{i=1}^{n}\left|\hat{y}_i - y_i\right| \tag{11}$$

where n is the total number of samples. y_i is the actual value of GDP density, and $\hat{y}_i$ is the predicted value of GDP density.

3.6 | Counterfactual Simulation for Evaluating Policy Impact

In order to effectively integrate the external policy shock into the DCA simulation, this study follows the method of Chen et al. (2019), integrating policy-related elements into the original overall development probability Pg, and then performing CA iteration to achieve a counterfactual simulation of GDP development density under the policy impact. The counterfactual overall development probability can be calculated as follows:

$$Pg_{cf} = Pg_{\mathrm{origin}} \times \frac{1+d}{d} \times \mathrm{Trend} \tag{12}$$

where d is the distance to policy-related elements. This term increases the development probability in areas close to the policy-related elements. Trend is a coefficient to control the amplitude impacts of policy-related elements in different land uses. The Trend coefficient for land uses unfavorable to economic development, such as forests, farmland, and water bodies, are set to 0.2. While the coefficient for those suitable for economic development, such as urban land, grassland, and unused land, are set to 1.0. This ensures that policies have a higher impact on the land suitable for economic development.

4 | Result

4.1 | Economic Growth Analysis in the Metropolitan Area

The actual economic growth of Wuhan metropolitan area from 2010 to 2020 is first analyzed based on the actual GDP data to reveal the general pattern. Figure 6B shows the relationship between the initial regional GDP and their corresponding growth in a decade, revealing a trend of the GDP growth-rate curve (red curve). The curve exhibits an upward trajectory when the initial GDP is relatively low. It attains its peak when the initial GDP reaches a specific threshold. Subsequently, as the initial GDP value rises, the growth rate of GDP declines gradually. This pattern fits the trend of the growth rate curve of the S-curve model (Figure 6A), which indicates that the GDP growth fits the growth-rate pattern of the S-curve model.

Table 1 presents the simulation accuracy metrics of the DCA model and the baseline models, clearly demonstrating that the DCA model has good performance in urban economic simulation both at the pixel and city levels. At the pixel level, the DCA model achieves substantial improvements across all three evaluation metrics compared to PLUS—a 13.87% relative reduction in RMSE, a 57.63% relative reduction in MAPE, and a 58.21% relative reduction in MAE. When benchmarked against the Gray-Cells CA model, the DCA model delivers notable enhancements—a 29.78% relative reduction in RMSE, a 7.03% relative reduction in MAPE, and an 18.41% relative reduction in MAE. Robustness analysis under the same settings (see Section S1 and Table S1 in the Supporting Information)

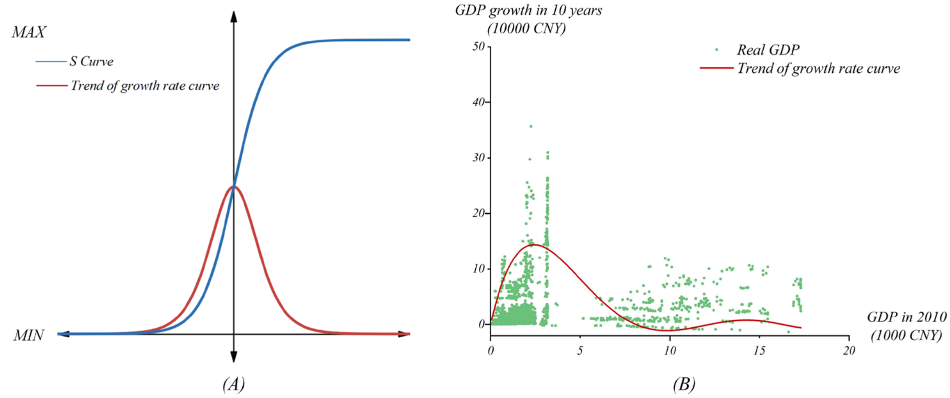

FIGURE 6 | Trend of GDP growth rate in the Wuhan metropolitan area. (A) Conceptual diagram of S-curve model. (B) Actual GDP data in the study area.

TABLE 1 | The simulation accuracy of different models at the pixel level and the city level.

Evaluation level	Model	RMSE (10,000 CNY/km^2)	MAPE %	MAE (10,000 CNY/km^2)
Pixel level	PLUS	13346.98	117.38	5426.81
	Gray-cells CA	16370.16	53.49	2779.60
	DCA	**11495.13**	**49.73**	**2267.85**
City level	ARIMA	865.57	**8.30**	434.29
	Random forest	999.15	16.18	628.71
	PLUS	5737.22	114.49	3693.68
	Gray-cells CA	3250.16	14.80	1424.75
	DCA	**546.55**	14.44	**377.33**

Note: Bold values indicate the best performance.

and across different temporal scopes (see Section S3 and Table S8) confirms the stability of the performance of the DCA model. These results demonstrate that the continuous-state mechanism of the DCA model integrated with the S-curve growth function robustly refines the precision of urban economic simulation compared to existing continuous-state CA frameworks. At the city level, the proposed DCA still outperforms all the baseline models, further showing its ability in simulating the spatial distribution of GDP.

Compared with the simulated GDP distributions by the baseline models, the DCA model has demonstrated its capacity to simulate the primary economic distribution within the central region of the Wuhan metropolitan area (Figure 7). While the PLUS model has the capacity to simulate the economic distribution of the central area of the Wuhan metropolitan area, it struggles to accurately simulate the economic distribution in areas farther from Wuhan, such as Qianjiang and Xianning. Although the gray-cells CA model performs well in simulating the overall economic distribution (Table 1), it inadequately simulates the economic distribution in the central area. Figure 7C shows that the simulated values appear overly smooth and lack the local variations and discontinuities that characterize the real economic distribution. In contrast, the result of the DCA model fits the pattern in the central region, as well as the complex economic distribution of the other eight non-core cities compared with the ground truth (Figure 7A,D). Therefore, the S-curve-based DCA is better suited to simulate the urban economy in metropolitan areas, which proves that the paradigm of evolutionary spatiotemporal dynamics is a more suitable theoretical framework for economic modeling than the geographic-determinism assumption.

4.2 | Details of the Implementation Results of Different Models

To investigate the simulation performance of DCA in different regions of the study area, the GDP of nine cities in the Wuhan metropolitan area for the year 2020 was simulated by diverse models (Figure 8). Compared with the PLUS model, DCA achieves the most significant MAPE reduction in Tianmen (Region 8), dropping 78.74% from 233.98% to 49.74% (Table 2). This is followed by Ezhou (Region 3) and Wuhan (Region 1), with MAPE reductions of 73.22% and 73.58% respectively. For RMSE, the largest improvement occurs in Wuhan, where DCA reduces the value by 20.03% from 31,574 to 25,250. In MAE, the most notable decrease is in Ezhou, with a 77.18% drop from 16,003 to 3651. Compared with the Gray-cells CA model, DCA reduces MAPE most significantly in Huangshi (Region 2) by 11.87% from 56.61% to 49.89%. For RMSE, the peak improvement is in Wuhan, with a 41.82% reduction from 43,399 to 25,250. In MAE, the largest decrease appears in Huangshi, dropping 18.18% from 2459 to 2012. The DCA model can show

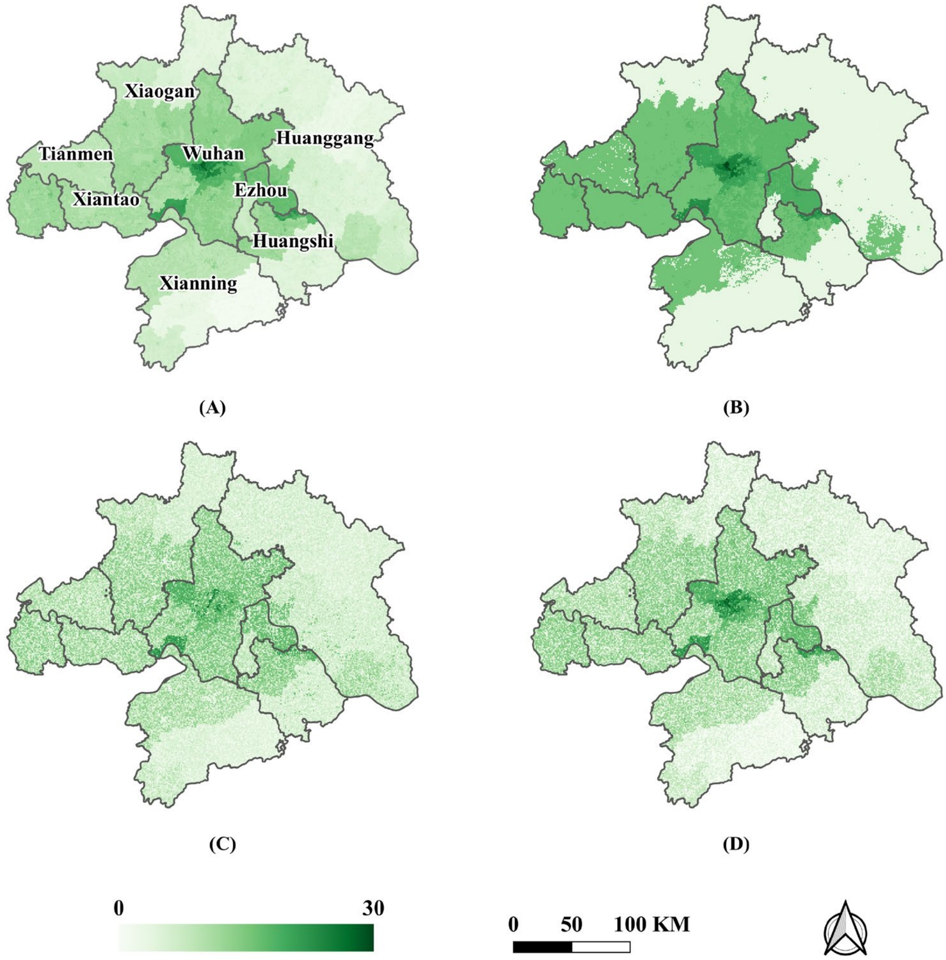

FIGURE 7 | Simulated GDP change (10,000 CNY per km2) in the Wuhan metropolitan area in 2020. (A) Truth growth. (B) PLUS. (C) Gray-cells CA. (D) The proposed DCA. The color-bar maximum of 300,000 CNY/km^2 is set solely for visualization to enhance spatial contrast. Grid cells with higher GDP densities are therefore displayed using the maximum color.

better simulation results for the economic distribution of the nine medium and large cities in the Wuhan metropolitan area compared to other models.

The Wuhan metropolitan area is gradually forming a dual-core structure with Wuhan City and the Ezhou-Huanggang-Huangshi region, promoting the integrated development of surrounding cities through transportation and economic integration. As shown in Figure 8 (A1)–(D1) and (A2)–(D2), the DCA model performs particularly well in these core areas. The DCA reduces the MAE by 27.83% in Wuhan City and by 8.45% to 18.18% in the Ezhou-Huanggang-Huangshi region, covering the range of reductions across cities in the region compared to the gray-cells CA model as a continuous simulation method. However, cities in the western and southern parts of the Wuhan metropolitan area, such as Xianning and Qianjiang, are weakly connected to the core area due to multiple factors, resulting in a generally low level of development and compactness of the urban agglomeration (CL Fang et al. 2018). This is further evidenced by the DCA model results, where the improvement in GDP simulation accuracy is relatively low in these areas, as seen in Figure 8 (D6) (D8), with only 3.86% and 7.28% improvements in Xianning and Tianmen, respectively. The central urban area of Wuhan and the Ezhou-Huanggang-Huangshi region are the core areas of the Wuhan metropolitan area, characterized by the fastest urbanization and high levels of urban spatial interaction (Jianhua He, Li, et al. 2017; Zhou et al. 2023).

To further explain the observed differences in simulation accuracy between core and peripheral areas, we conducted an error–context analysis along a representative profile crossing the Wuhan metropolitan area (Figure 9A). Along this profile, we delineated Region 1 as the Wuhan core area, Region 2 as the core area of the Ezhou–Huangshi region, and Region 3 as the remaining areas along the profile excluding Regions 1 and 2. Figure 9B plots the absolute prediction errors of different models along the profile, showing pronounced errors that peak in the urban area of Wuhan, and the second highest peak in the Ezhou-Huanggang-Huangshi region, while Region 3 generally exhibits lower and more stable errors. We then quantified two key factors closely related to transportation accessibility and human activity intensity: road network density and POI density. As shown in Figure 9C, Region 1 has the highest road network density across all kinds of road, followed by Region 2, whereas Region 3 has the lowest density. In addition, POI density exhibits a highly uneven spatial pattern (Figure 9D), with Region 1 reaching 172.30 unit/km^2, substantially higher than Region 2 (21.80 unit/km^2) and Region 3 (6.55 unit/km^2). These results indicate that the two core areas along the profile are characterized

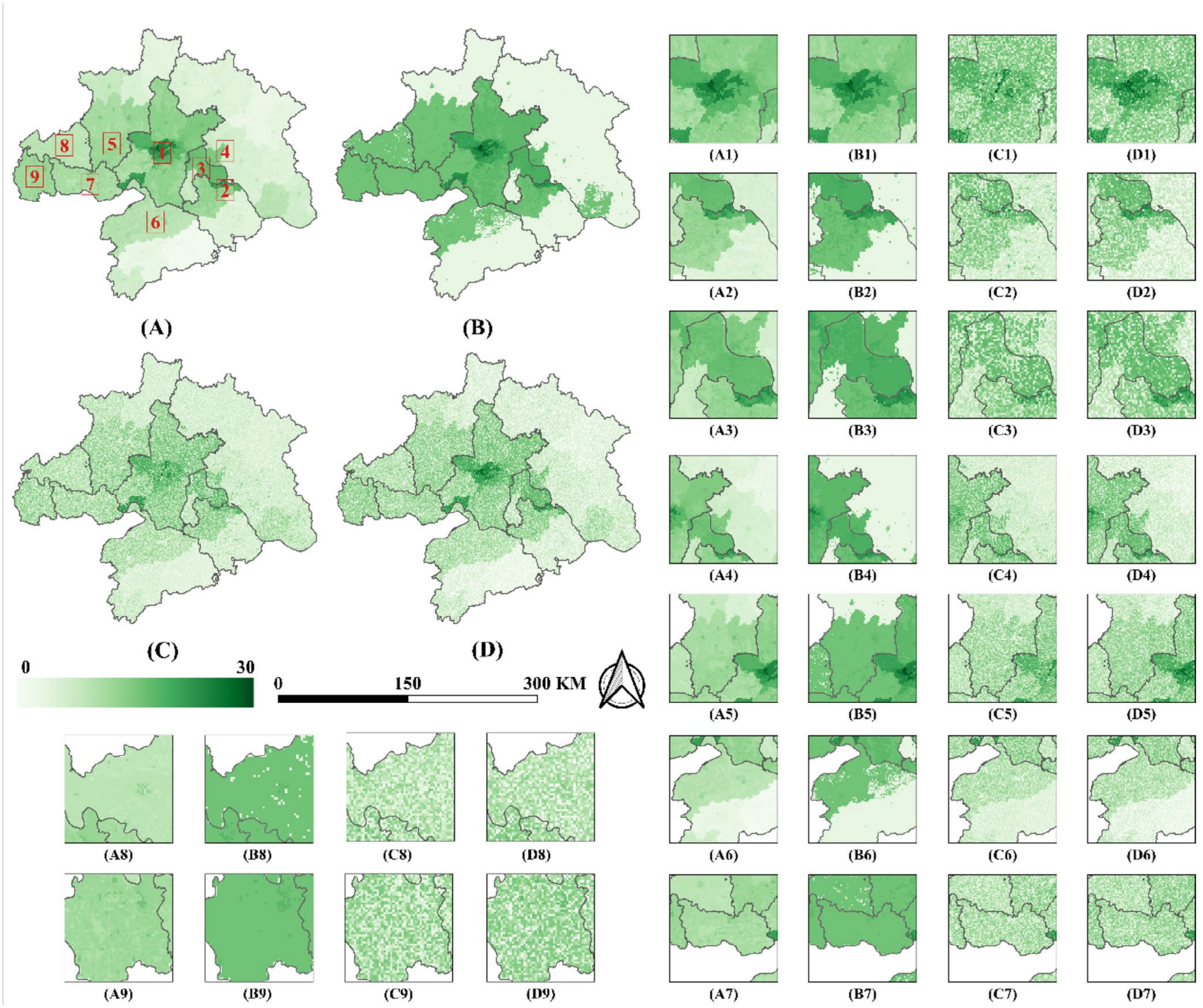

FIGURE 8 | Detailed simulated GDP changes (10,000 CNY per km2) in Wuhan metropolitan area in 2020. Region 1~9 are representative examples in Wuhan, Huangshi, Ezhou, Huanggang, Xiaogan, Xianning, Xiantao, Tianmen and Qianjiang, respectively. (A) Ground truth. (B) PLUS. (C) Gray-cells CA. (D) DCA. (A1~A9) Ground truth in the 9 representative regions. (B1~B9) Simulated results by PLUS model in the 9 representative regions. (C1~C9) Simulated results by gray-cells CA model in the 9 representative regions. (D1~D9) Simulated results by the proposed DCA model in the 9 representative regions. The color-bar maximum of 300,000 CNY/km^2 is set solely for visualization to enhance spatial contrast. Grid cells with higher GDP densities are therefore displayed using the maximum color.

by stronger accessibility and more intensive and diverse socio-economic activities.

The coincidence of higher errors with higher road/POI densities suggests that model accuracy is negatively affected in highly urbanized areas where land-use dynamics are more complex. In particular, the Wuhan core area and the Ezhou-Huangshi core area concentrate population, infrastructure, and industrial/service functions, and typically experience more frequent infill development, redevelopment, and mixed land-use transitions, leading to higher spatial fragmentation and stronger nonlinear interactions among drivers. In contrast, Region 3 is dominated by relatively stable land-use types and slower change processes, which are easier for CA-based models to reproduce, resulting in lower errors. This pattern reflects the metropolitan urban–rural dual structure and the strong concentration of resources and accessibility advantages in core areas, which jointly amplify land-change complexity and thus simulation uncertainty.

4.3 | Analysis of the Impact of the Metropolitan Master Plan

This study employs counterfactual simulations to assess the impact of regional coordinated development policies on the economic growth of the Wuhan metropolitan area. The regional spatial structure, as delineated in the Wuhan Metropolitan Area Master Plan (NDRC 2009), was incorporated into the DCA model to simulate GDP distribution. The objective is to evaluate the effectiveness of regional coordinated development policies by addressing the following question: Assuming

TABLE 2 | The simulation accuracy of different models in the Wuhan metropolitan area.

City	PLUS			Gray-cells CA			DCA		
	MAPE %	RMSE (10,000 CNY/km^2)	MAE (10,000 CNY/km^2)	MAPE %	RMSE (10,000 CNY/km^2)	MAE (10,000 CNY/km^2)	MAPE %	RMSE (10,000 CNY/km^2)	MAE (10,000 CNY/km^2)
Wuhan	188.61	31,574	17,979	54.99	43,399	11,320	**49.82**	**25,250**	**8170**
Huangshi	97.17	10,248	4617	56.61	9359	2459	**49.89**	**6054**	**2012**
Ezhou	189.16	19,710	16,003	53.08	6125	3988	**50.66**	**5009**	**3651**
Huanggang	71.84	3045	1340	53.88	1208	748	**49.97**	**1088**	**680**
Xiaogan	101.12	4258	3137	52.24	1982	1400	**49.33**	**1743**	**1286**
Xianning	105.38	3708	2468	51.03	1268	855	**50.14**	**1145**	**822**
Xiantao	158.89	5459	5315	53.96	2455	1871	**50.10**	**1718**	**1718**
Tianmen	233.98	6005	5852	53.32	1667	1346	**49.74**	**1456**	**1248**
Qianjiang	124.46	5180	4888	54.06	2715	2183	**49.28**	**2329**	**1978**

Note: Bold values indicate the best performance.

the regional spatial structure of the Wuhan metropolitan area had been implemented in 2010 in accordance with the master plan, what would have been the resultant variation in GDP distribution compared with the actual outcome in 2020? The Wuhan Metropolitan Area Master Plan emphasizes a regional spatial structure centered on Wuhan, driving the development of surrounding cities, which manifests in the key transportation elements portraited in Figure 10A, including ring roads, expressways, and railways. Moreover, the master plan mentions four cooperative groups, i.e., the Huangshi-Ezhou-Huanggang group, the Xiantao-Qianjiang-Tianmen group, the Xiaogan-Hanchuan-Yingcheng group, and the Xianning-Chibi-Jiayu group, which are also portraited in Figure 10A. Based on these key elements, the counterfactual GDP in 2020 is simulated (Figure 10B).

The counterfactual simulation in Table 3 shows that, compared to the baseline scenario, the completion of the policy-related elements increased the simulated GDP by 2,503,271 CNY in 2020 (a relative growth rate of 0.96%). This suggests the overall positive impact of regional coordinated development on the macroeconomy, which is highly consistent with the classic theoretical expectation that transportation infrastructure guides regional development.

However, the spatial distribution of these policy dividends exhibits strong regional heterogeneity. High-density growth areas are concentrated in Wuhan's main urban area and along the Ezhou-Huanggang-Huangshi intercity railway and expressway, forming a significant polarized cluster (Figure 10C,D1). Wuhan, as the central hub of the planned road network, benefited most from this policy dividend due to its strong industrial base, comprehensive public services, and powerful factor attraction capabilities. Its GDP increased by an absolute amount of 2,521,516.72 yuan, with a relative growth rate of 1.76%, far exceeding the average level of urban clusters. The growth of node cities along the main lines of the planned road network (Wuhan-Ezhou-Huanggang-Huangshi, Wuhan-Xianning, and Wuhan-Xiaogan corridors) was particularly prominent. The relative growth rates of Huangshi, Xiaogan, Xianning, Ezhou, and Qianjiang were 0.90%, 0.73%, 0.66%, 0.40%, and 0.30%, respectively. Huangshi, due to improved efficiency in industrial cooperation with Wuhan and the absorption of a large amount of industrial spillover, became the fastest-growing city outside of Wuhan.

Besides being scattered around the outskirts of Wuhan's main urban area, areas experiencing negative high-density reductions also showed a significant negative growth of less than 3% in the Tianxianqian cluster and Huanggang region (Figure 10E,F1,F2). This indicates that areas far from core transportation axes or with weaker inherent competitiveness are having their resources "siphoned off" by strong transportation corridors. However, the overall trend does not affect the conclusion that the planned road network has a positive overall driving effect on the regional economy. The observed GDP reduction in some peripheral cities under the counterfactual scenario results from the combined effects of development probability redistribution and neighborhood competition. Specifically, the enhanced transportation corridors directly increase the development probability P_g^{cf} of cells located near major accessibility corridors, serving as the primary policy-transmission mechanism. Hence, cells close to policy-related transportation elements and associated with development-suitable land uses receive relatively higher probabilities, while isolated cells and cells assigned lower Trend values may receive lower probabilities than under the baseline scenario. Subsequently, the neighborhood interaction term Ω_i, as a local spatial amplification mechanism, reinforces this pattern because cells surrounded by higher-density development obtain larger growth increments (Zhang et al. 2023). Therefore, the observed decline in peripheral cities reflects a redistribution of future development opportunities.

4.4 | Sensitivity Analysis of Zoning Settings for DCA

Based on the DCA model, this study examined the scale effect of zoning settings on urban economic simulation. CA models have been demonstrated to be sensitive to the size of the modeling

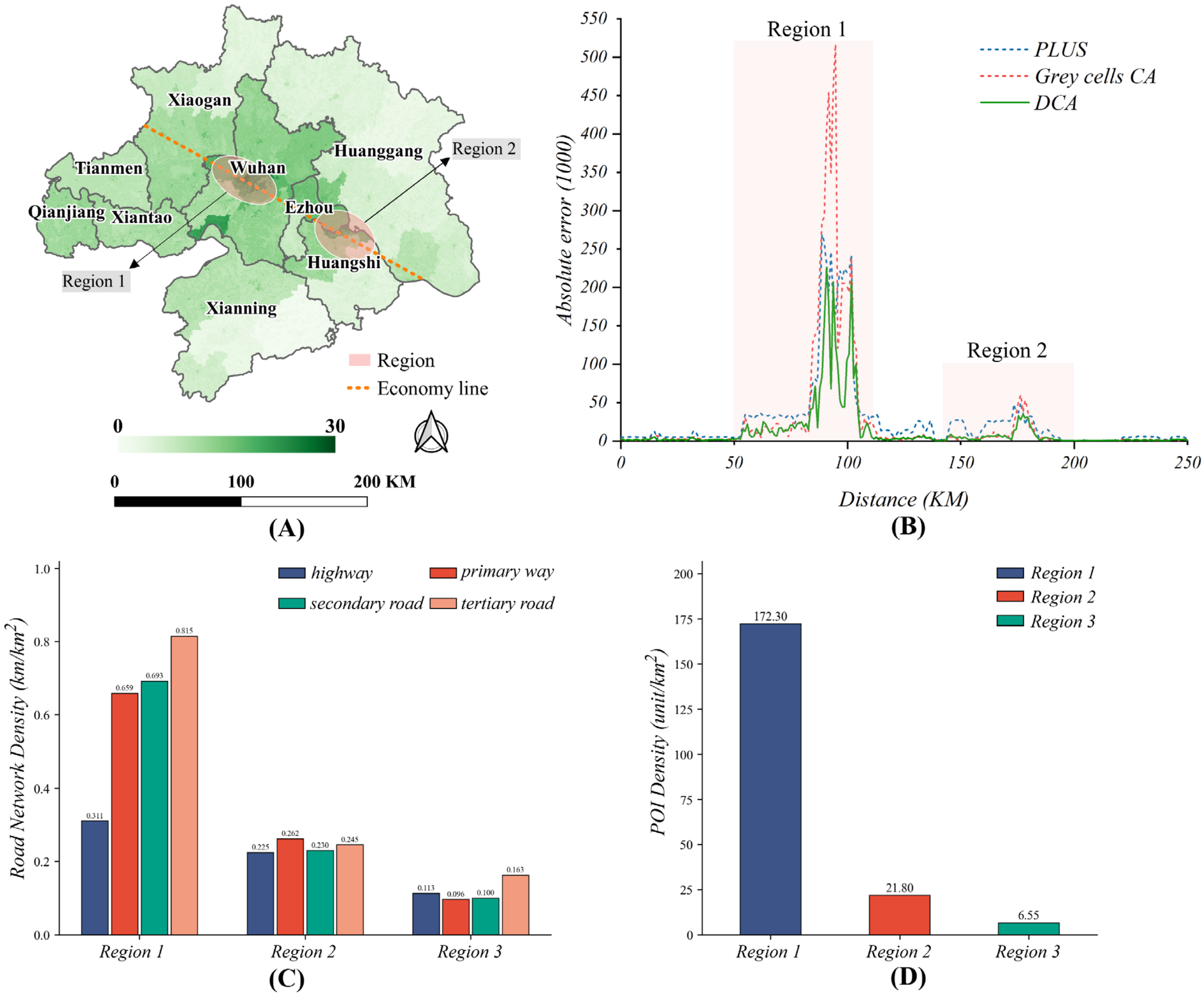

FIGURE 9 | Profile analysis. (A) Spatial distributions of GDP in 2020 and the economic line. (B) Absolute errors of the simulation results by different models along the profile. (C) Comparison of the road network densities in the different regions. Region 1 is the Wuhan core area while Region 2 refers to the core area of Ezhou–Huangshi region. Region 3 refers to the remaining areas along the profile, excluding Region 1 and Region 2. (D) Comparison of POI density in the different regions.

area (Wu et al. 2019). In this study, the zoning settings are based on administrative divisions, including municipal and county-level boundaries, with two-fold reasons. (1) GDP is fundamentally compiled and officially reported following administrative jurisdictions. And (2) economic growth and spatial development are strongly shaped by jurisdiction-specific policy instruments, which are typically enacted within administrative boundaries. Our results indicate that using county-level administrative divisions to delineate the study area can effectively improve the simulation accuracy in terms of RMSE and MAE (Figure 11). Figure 11A2 shows that MAPE varies within a ±1% range, with an overall decrease of 0.19% using the county-level division methodology. Figure 11C2 shows that MAE varies within a ±200 range, with an overall improvement of 78.98 using the county-level division methodology. RMSE varied within a ±2000 range, with Wuhan city's RMSE accuracy improving by 1613.41 and the overall metropolitan area improving by 2084.51 using the county-level division methodology in Figure 11B2. The simulation results indicate that using more detailed regional divisions has a minor impact on MAPE. However, detailed regional divisions have a significant impact on RMSE and MAE. Overall, this regional divisions reduces the simulation error and improves the accuracy of GDP simulations for the Wuhan metropolitan area.

We also conducted parameter sensitivity analyses for other key parameters that are related to input data, algorithmic, and spatial mechanisms of DCA, including the sampling rate, the number of decision trees, the neighborhood size, and the cell radius (Table S2). Tables S3–S6 indicate that the settings of all key parameters achieved local optima. Please check Section S2 in the Supporting Information for detailed analysis.

5 | Discussion

This paper proposes a DCA model that integrates the S-curve and the CA paradigm to provide an alternative continuous-state CA model for simulating urban continuous variables. DCA

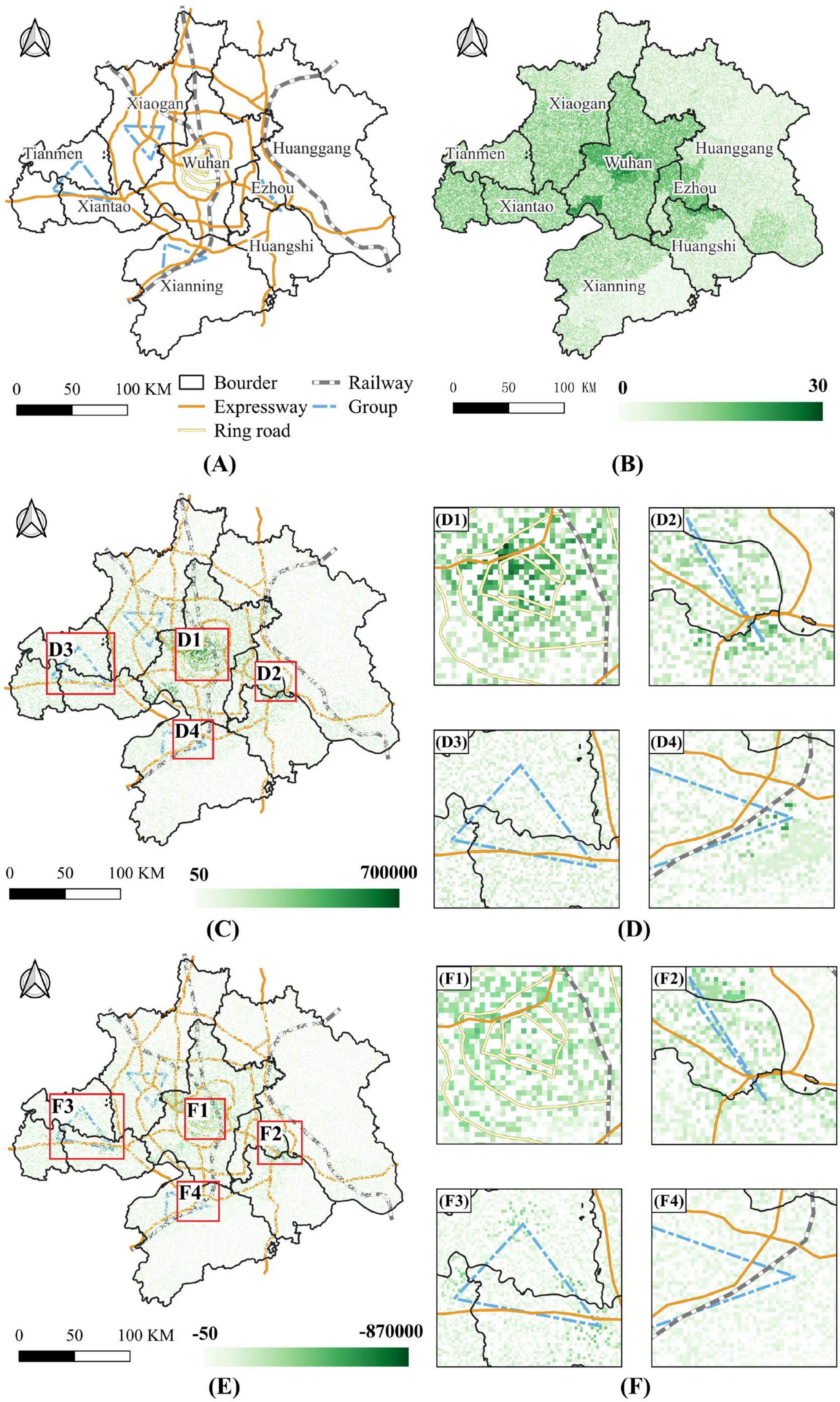

FIGURE 10 | Legend on next page.

FIGURE 10 | Counterfactual simulation to assess the impact of regional coordinated development policies. (A) Key elements reflecting the regional spatial pattern mentioned in the master plan include ring roads, expressways, railways, and four cooperative subgroups. (B) Counterfactual GDP distribution under the impact of the master plan in 2020 (Unit: 10,000 CNY/km^2). (C) Positive difference comparing to the actual GDP distribution (Unit: CNY/km^2). The grids with a difference under 50 CNY were filtered to better showcase spatial trends. (E) Negative difference comparing to the actual GDP distribution (Unit: CNY/km^2). The grids with a difference above −50 CNY were filtered to better showcase spatial trends. (D) and (F) show the spatial details of the differences of (counterfactual GDP—actual GDP). (D1, F1: Wuhan main urban area; D2, F2: Ezhou-Huangshi-Huanggang group; D3, F3: Tianmen-Xiantao-Qianjiang group; D4, F4: Xianning group).

TABLE 3 | Comparison of simulated GDP in 2020 across cities under baseline and counterfactual scenarios (unit: CNY).

City	Baseline GDP	Counterfactual GDP	Absolute change	Growth rate %
Wuhan	143,404,502.47	145,926,019.19	2,521,516.72	1.76
Huangshi	18,779,490.05	18,949,032.03	169,541.98	0.90
Xiaogan	23,196,963.51	23,366,118.83	169,155.32	0.73
Xianning	15,927,082.87	16,032,228.91	105,146.04	0.66
Ezhou	11,842,143.34	11,889,376.82	47,233.48	0.40
Qianjiang	8,004,026.00	8,027,997.26	23,971.26	0.30
Tianmen	6,514,312.52	6,490,194.24	−24,118.28	−0.37
Huanggang	23,681,661.74	23,393,061.00	−288,600.74	−1.22
Xiantao	8,486,536.08	8,265,961.75	−220,574.33	−2.60
Total	259,836,718.58	262,339,990.03	2,503,271.45	0.96

introduces the S-curve, revealing the complex distribution pattern of the metropolitan area economy in the real world. This method significantly improves the accuracy of the economic simulation. The framework examines the urban economy from a dynamic research perspective, provides new ideas for urban economic simulation, and helps to capture urban economic development trends and patterns more accurately.

The proposed DCA model was applied to simulate the GDP of the Wuhan metropolitan area, revealing the complex economic growth patterns of metropolitan areas. A data-driven finding shows that economic growth follows an S-curve trend. Our results indicate that the S-curve-based DCA model shows good performance (Table 1) and robustness (Table S1). Compared to the discrete-state PLUS model, our model reduces MAE by 58.21%. While it lowers RMSE by 29.78% compared to the conventional continuous-state Gray-Cells CA model. The DCA model has been demonstrated to possess a superior capacity to simulate the intricate distribution of the urban economy, particularly in contexts characterized by elevated economic complexity. The conventional continuous-state Gray-Cells CA model outperforms the discrete-state PLUS model, exhibiting a MAPE of 53.49%, as opposed to the PLUS model's 117.38%. Nonetheless, its RMSE is 22.65% higher than that of PLUS, a discrepancy attributable to the presence of outliers. The Wuhan metropolitan area exhibits a trend of coexisting multiple centers (Jing et al. 2018), and treating it as a single entity for economic simulation will result in many outliers. Furthermore, cross-time validation results from 2000 to 2010 and 2010 to 2020 show that both the accuracies of the DCA model are far higher than those of the two baseline models (Table S8), demonstrating the excellent stability of DCA across different time spans. This characteristic provides crucial support for the model's application in long-term economic simulations and its ability to withstand uncertainties in the time dimension.

By analyzing the differences in economic growth among different cities within the metropolitan area, this study reveals the distribution patterns of economic growth in these cities, providing support for economic development policies in the metropolitan area. DCA exhibits better simulation effects in urban edge areas. However, this improvement in simulation accuracy varies across different regions. In the core areas of the metropolitan area, the improvement in accuracy is the most significant. According to the analysis, the areas with strong links to the core cities of the metropolitan area have a higher level of economic development and better economic simulations. In contrast, in the peripheral areas of the Wuhan metropolitan area such as Xianning city and Tianmen city, the improvement in GDP simulation accuracy is relatively low. These areas have more mountainous areas and are farther away from Wuhan City, resulting in a slower growth rate in their economy. In conclusion, the methodology presented in this paper is more applicable to regions with a higher level of economic integration in metropolitan areas. DCA aids in better understanding the interconnections and impacts between cities within the metropolitan area. Our results indicate that the urban managers of the Wuhan metropolitan area are suggested to focus on strengthening the connections between different cities, promoting the economic integration of the metropolitan area. This understanding facilitates the formulation of more effective policy measures to promote the rational allocation and optimal utilization of resources (X. Gao et al. 2020).

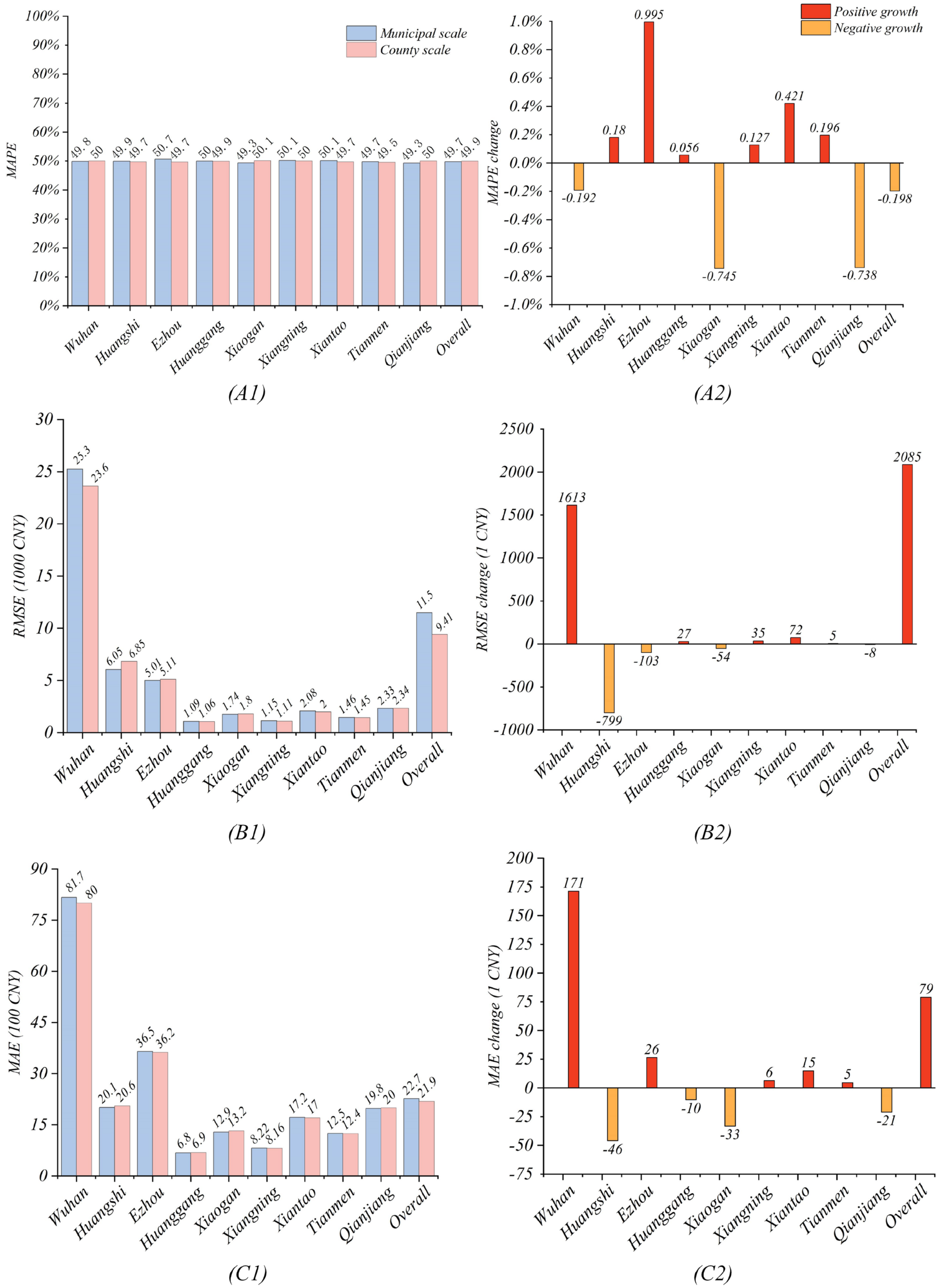

FIGURE 11 | Accuracy of DCA economic simulation results for different cities at the municipal and county levels. (A1~A2) Comparison of MAPE and changes. (B1~B2) Comparison of RMSE and changes. (C1~C2) Comparison of MAE and changes.

Based on the comparative analysis of the counterfactual and baseline scenarios, this study proposes specific policy recommendations in the following three dimensions: (1) In the implementation of the master plan, the underlying constraint of land use must be leveraged. We recommend that the government, based on the forecast results, reserve and prioritize land supply suitable for industrial and commercial development in high-growth potential areas along transportation corridors. Simultaneously, for peripheral areas with weak road network coverage, such as Tianmen and Qianjiang, it is crucial to improve transportation network connectivity to reduce commuting time and distance. (2) In regions with simulated medium-to-high growth, the construction of core transportation corridors should be firmly promoted to maximize the radiation range and agglomeration effect of policy dividends. Wuhan should further strengthen its industrial spillover capacity as a core hub, prioritizing the layout of industrial transfer receiving parks at road network intersections and along core corridors. Industrial division of labor and cooperation with high-response node cities such as Huangshi, Ezhou, and Xiaogan should be promoted. (3) The simulation results warn that in economically damaged regions, simplistic spatial planning and rapid infrastructure development can exacerbate factor outflow. These regions experience a “siphoning effect” and a decline in economic density during regional integration development. Therefore, it is recommended that these regions simultaneously introduce non-spatial constraint policies as compensation to achieve true Pareto optimality at the metropolitan area level.

This study explored the scale effect of zoning units on DCA model performance, revealing that finer administrative units significantly enhance simulation fidelity in metropolitan economic forecasting. The results demonstrate that smaller analytical units improve spatial accuracy by capturing intra-city heterogeneity, whereas coarse unit delineations compromise prediction precision—potentially leading to ineffective or misaligned policy interventions. Economic distribution within the metropolitan area is complex and variable. Dividing the metropolitan area into multiple regions can effectively improve the simulation accuracy of the urban economy. Despite the negligible impact of regional division scale (municipal vs. county-level) on MAPE, it improves MAE by 78.98 and reduces overall RMSE by 15.35% when using county-level divisions instead of municipal-level ones. The RMSE metric is sensitive to outliers in the data, thereby affecting the accuracy of the model (Chai and Draxler 2014). This empirical evidence highlights that metropolitan economies exhibit complex, variable distributions, where non-core cities increasingly influence regional dynamics (Charron et al. 2015). Consequently, detailed spatial partitioning mitigates outlier distortions and stabilizes simulations—an essential advancement for urban development planning to address evolving economic interconnectivity and accurately model peripheral city contributions.

Further refinements are still required on several fronts. This study uses 2018-derived POI and spatial auxiliary data to simulate 2020 GDP density, a choice justified by two practical considerations: (1) Core spatial drivers in the Wuhan metropolitan area (e.g., road networks, commercial POI distributions) showed minimal changes between 2018 and 2020, as major infrastructure projects and land-use adjustments were largely completed by 2018; (2) 2018 is the most recent year for which high-quality, full-coverage POI data were publicly available at the time of study. Despite this rationale, temporal mismatch may introduce potential biases: short-term, post-2018 events (e.g., temporary policy incentives for industrial relocation, small-scale infrastructure upgrades) are not captured, which could lead to slightly overestimated or underestimated simulation accuracy in peripheral areas with rapid, recent changes. Moreover, the LULC and GDP datasets have inherent errors in their generation process, which is an issue that is not susceptible to being circumvented by data science. However, the core mechanism of the CA model suppresses the propagation and amplification of errors (Yeh and Li 2006). On the one hand, the neighborhood averaging effect of the CA model can smooth the data source error of a single cell. On the other hand, the dynamic correction of cell states during the model's iterative process further reduces the accumulation of uncertainty. In addition, with the advancement of urbanization in the Wuhan metropolitan area, the area of developable land is gradually decreasing, and the spatial constraints on urban development are increasing, which also limits the free propagation of errors to some extent. The robustness of the DCA model shows the rule-based mechanism of CA enables economic simulation to converge, thereby offering a more accurate reflection of the objective laws of urban economic development, as opposed to the cumulative effect of data errors.

A further limitation is that the independently calibrated S-curves assume temporally invariant parameters within each administrative unit. In particular, the asymptotic GDP-density parameter x_m reflects the long-term development regime inferred from historical observations. A major structural intervention, such as a large-scale industrial relocation policy, may increase x_m in receiving regions and decrease it in regions experiencing industrial out-migration. Similarly, a prolonged recession accompanied by permanent losses in productive capacity may reduce the effective x_m, whereas a temporary recession may mainly delay the convergence process by affecting the growth-rate parameter $\boldsymbol{r}$. Because the current framework does not update these parameters endogenously, projections following such shocks may systematically deviate from the observed trajectory.

In future research, more potential factors can be introduced based on actual research scenarios to simulate the urban regional growth patterns more realistically. Based on the actual conditions of the research area and the city development density, an appropriate zoning method should be selected to achieve a high-precision simulation of the complex economic distribution within the metropolitan area. Another important future research direction is long-term economic forecasting. Currently, DCA assumes the actual overall economic output, the asymptotic maximum GDP density, and the growth rate of GDP density to remain constant. However, how to reliably predict future regional overall economic output remains unclear. Therefore, future research could consider incorporating future economic output forecasting models into the DCA model.

6 | Conclusion

This study proposes an urban economic simulation framework based on Density Cellular Automata integrating with the S-curve model, facing the challenge of simulating urban economic evolution with fine-grained spatial information. The framework models the urban economy from a spatial and temporal perspective and introduces an S-curve model in terms of economic growth. The results show that regional economic growth follows the S-shaped trend, revealing the complex economic distribution within metropolitan areas and enhancing simulation accuracy. The connection between cities is fortified as urbanization and economic development advance. Non-core cities within metropolitan areas are progressively assuming a more substantial role in the broader metropolitan economy. A potential suggestion based on our results indicates that the Hubei provincial government may consider focusing on the economic growth trends of different cities and analyzing the key factors that limit their growth in order to enhance economic development. Additionally, it would also be advisable to balance urbanization with ecological sustainability and promote green city construction. The proposed DCA model is helpful to enhance the understanding of the complex distribution of the urban economy on both temporal and spatial dimensions. The revealed patterns can also provide a reference for urban planning-related departments to formulate development plans.

Acknowledgments

This work was supported by the Open Fund of Key Laboratory of Urban Land Resources Monitoring and Simulation, Ministry of Natural Resources [KF-2023-08-04], as well as the National Natural Science Foundation of China [42471491] [42171466] and "CUG Scholar" Scientific Research Funds at China University of Geosciences (Wuhan) [2022034]. Open Access funding enabled and organized by Projekt DEAL.

Funding

This work was supported by Open Fund of Key Laboratory of Urban Land Resources Monitoring and Simulation, Ministry of Natural Resources, KF-2023-08-04. National Natural Science Foundation of China, 42471491, 42171466. "CUG Scholar" Scientific Research Funds at China University of Geosciences (Wuhan), 2022034.

Conflicts of Interest

The authors declare no conflicts of interest.

Data Availability Statement

The DCA software mentioned in the study is released on Figshare at https://figshare.com/s/72676d9aa35e6068f669. Demo data and user documentation are also available. The source codes and data for replicating research results are also provided at https://figshare.com/s/77762795a32b0d979fb6.

References

Abonazel, M. R., and A. I. Abd-Elftah. 2019. "Forecasting Egyptian GDP Using ARIMA Models." *Reports on Economics and Finance* 5, no. 1: 35–47.

Baker, D., R. Merkert, and M. Kamruzzaman. 2015. "Regional Aviation and Economic Growth: Cointegration and Causality Analysis in Australia." *Journal of Transport Geography* 43: 140–150.

Cao, Y., X. Zhang, Y. Fu, Z. Lu, and X. Shen. 2020. "Urban Spatial Growth Modeling Using Logistic Regression and Cellular Automata: A Case Study of Hangzhou." *Ecological Indicators* 113: 106200. https://doi.org/10.1016/j.ecolind.2020.106200.

Chai, T., and R. R. Draxler. 2014. "Root Mean Square Error (RMSE) or Mean Absolute Error (MAE)? –Arguments Against Avoiding RMSE in the Literature." *Geoscientific Model Development* 7, no. 3: 1247–1250. https://doi.org/10.5194/gmd-7-1247-2014.

Chakraborty, A., S. Sikder, H. Omrani, and J. Teller. 2022. "Cellular Automata in Modeling and Predicting Urban Densification: Revisiting the Literature Since 1971." *Land* 11, no. 7: 1113. https://doi.org/10.3390/land11071113.

Charron, N., L. Dijkstra, and V. Lapuente. 2015. "Mapping the Regional Divide in Europe: A Measure for Assessing Quality of Government in 206 European Regions." *Social Indicators Research* 122: 315–346.

Chen, D., Y. Zhang, Y. Yao, Y. Hong, Q. Guan, and W. Tu. 2019. "Exploring the Spatial Differentiation of Urbanization on Two Sides of the Hu Huanyong Line–Based on Nighttime Light Data and Cellular Automata." *Applied Geography* 112: 102081.

Clarke, K. C., and L. J. Gaydos. 1998. "Loose-Coupling a Cellular Automaton Model and GIS: Long-Term Urban Growth Prediction for San Francisco and Washington/Baltimore." *International Journal of Geographical Information Science* 12, no. 7: 699–714.

Dahiya, B. 2014. "Southeast Asia and Sustainable Urbanization." *Global Asia* 9, no. 3: 84–91.

Fang, C., Z. Wang, and H. Ma. 2018. "The Theoretical Cognition of the Development Law of China's Urban Agglomeration and Academic Contribution." *Acta Geographica Sinica* 73, no. 4: 651–665.

Fang, C., and D. Yu. 2017. "Urban Agglomeration: An Evolving Concept of an Emerging Phenomenon." *Landscape and Urban Planning* 162: 126–136.

Gao, K., Y. Yang, A. Li, and X. Qu. 2021. "Spatial Heterogeneity in Distance Decay of Using Bike Sharing: An Empirical Large-Scale Analysis in Shanghai." *Transportation Research Part D: Transport and Environment* 94: 102814. https://doi.org/10.1016/j.trd.2021.102814.

Gao, X., A. Zhang, and Z. Sun. 2020. "How Regional Economic Integration Influence on Urban Land Use Efficiency? A Case Study of Wuhan Metropolitan Area, China." *Land Use Policy* 90: 104329. https://doi.org/10.1016/j.landusepol.2019.104329.

He, J., C. Li, Y. Yu, Y. Liu, and J. Huang. 2017. "Measuring Urban Spatial Interaction in Wuhan Urban Agglomeration, Central China: A Spatially Explicit Approach." *Sustainable Cities and Society* 32: 569–583.

He, J., S. Wang, Y. Liu, H. Ma, and Q. Liu. 2017. "Examining the Relationship Between Urbanization and the Eco-Environment Using a Coupling Analysis: Case Study of Shanghai, China." *Ecological Indicators* 77: 185–193.

Hoshovska, O., Z. Poplavska, N. Kryvinska, and N. Horbal. 2020. "Considering Random Factors in Modeling Complex Microeconomic Systems." *Mathematics* 8, no. 8: 1206.

Hu, L., K. Tian, X. Wang, and J. Zhang. 2012. "The "S" Curve Relationship Between Export Diversity and Economic Size of Countries." *Physica A: Statistical Mechanics and its Applications* 391, no. 3: 731–739.

Jiao, L. 2015. "Urban Land Density Function: A New Method to Characterize Urban Expansion." *Landscape and Urban Planning* 139: 26–39.

Jing, Y., Y. Liu, E. Cai, Y. Liu, and Y. Zhang. 2018. "Quantifying the Spatiality of Urban Leisure Venues in Wuhan, Central China–GIS-Based Spatial Pattern Metrics." *Sustainable Cities and Society* 40: 638–647.

Ke, X., X. Wang, H. Guo, C. Yang, Q. Zhou, and A. Mougharbel. 2021. "Urban Ecological Security Evaluation and Spatial Correlation Research—Based on Data Analysis of 16 Cities in Hubei Province of China." *Journal of Cleaner Production* 311: 127613. https://doi.org/10.1016/j.jclepro.2021.127613.

Liang, X., Q. Guan, K. C. Clarke, S. Liu, B. Wang, and Y. Yao. 2021. "Understanding the Drivers of Sustainable Land Expansion Using a

Patch-Generating Land Use Simulation (PLUS) Model: A Case Study in Wuhan, China." *Computers, Environment and Urban Systems* 85: 101569.

Liu, J., and J. Diamond. 2005. "China's Environment in a Globalizing World." *Nature* 435, no. 7046: 1179–1186. https://doi.org/10.1038/4351179a.

Liu, X., G. Hu, B. Ai, et al. 2018. "Simulating Urban Dynamics in China Using a Gradient Cellular Automata Model Based on S-Shaped Curve Evolution Characteristics." *International Journal of Geographical Information Science* 32, no. 1: 73–101. https://doi.org/10.1080/13658816.2017.1376065.

Liu, Y., M. Batty, S. Wang, and J. Corcoran. 2021. "Modelling Urban Change With Cellular Automata: Contemporary Issues and Future Research Directions." *Progress in Human Geography* 45, no. 1: 3–24.

Liu, Y., T. Luo, Z. Liu, X. Kong, J. Li, and R. Tan. 2015. "A Comparative Analysis of Urban and Rural Construction Land Use Change and Driving Forces: Implications for Urban–Rural Coordination Development in Wuhan, Central China." *Habitat International* 47: 113–125. https://doi.org/10.1016/j.habitatint.2015.01.012.

Liu, Z., D. Guan, S. Moore, H. Lee, J. Su, and Q. Zhang. 2015. "Climate Policy: Steps to China's Carbon Peak." *Nature* 522, no. 7556: 279–281. https://doi.org/10.1038/522279a.

Luo, R., and D. He. 2023. "The Dynamic Impact of Land Use Change on Ecosystem Services as the Fast GDP Growth in Guiyang City." *Ecological Indicators* 157: 111275. https://doi.org/10.1016/j.ecolind.2023.111275.

Mahtta, R., M. Fragkias, B. Güneralp, et al. 2022. "Urban Land Expansion: The Role of Population and Economic Growth for 300+ Cities." *npj Urban Sustainability* 2, no. 1: 5. https://doi.org/10.1038/s42949-022-00048-y.

Mustafa, A., A. Heppenstall, H. Omrani, I. Saadi, M. Cools, and J. Teller. 2018. "Modelling Built-Up Expansion and Densification With Multinomial Logistic Regression, Cellular Automata and Genetic Algorithm." *Computers, Environment and Urban Systems* 67: 147–156. https://doi.org/10.1016/j.compenvurbsys.2017.09.009.

NDRC. 2009. "Wuhan Metropolitan Area Master Plan." https://fgw.hubei.gov.cn/fbjd/xxgkml/ghjh/lsgh/qt/201703/t20170327_1543776.shtml.

Peters, G. 2001. "A Linear Forecasting Model and Its Application to Economic Data." *Journal of Forecasting* 20, no. 5: 315–328.

Sezer, O. B., M. U. Gudelek, and A. M. Ozbayoglu. 2020. "Financial Time Series Forecasting With Deep Learning: A Systematic Literature Review: 2005–2019." *Applied Soft Computing* 90: 106181.

Siedlecki, R., D. Papla, and A. Bem. 2018. "Application of S-curve and Modified S-curve in Transition Economies' GDP Forecasting. Visegrad Four Countries Case." Paper presented at the Contemporary Trends and Challenges in Finance: Proceedings from the 3rd Wroclaw International Conference in Finance.

Sng, H. Y. 2010. *Economic Growth and Transition: Econometric Analysis of Lim's S-Curve Hypothesis*. Vol. 1. World Scientific.

Tian, Y. 2020. "Mutualistic Pattern of Intra-Urban Agglomeration and Impact Analysis: A Case Study of 11 Urban Agglomerations of Mainland China." *ISPRS International Journal of Geo-Information* 9, no. 10: 565.

Tu, W., W. Gao, M. Li, et al. 2024. "Spatial Cooperative Simulation of Land Use-Population-Economy in the Greater Bay Area, China." *International Journal of Geographical Information Science* 38, no. 2: 381–406. https://doi.org/10.1080/13658816.2023.2285459.

Wang, A., G. Wang, Q. Chen, W. Yu, K. Yan, and H. Yang. 2015. "S-Curve Model of Relationship Between Energy Consumption and Economic Development." *Natural Resources Research* 24: 53–64.

Willmott, C. J., and K. Matsuura. 2005. "Advantages of the Mean Absolute Error (MAE) Over the Root Mean Square Error (RMSE) in Assessing Average Model Performance." *Climate Research* 30, no. 1: 79–82.

Wu, H., Z. Li, K. C. Clarke, et al. 2019. "Examining the Sensitivity of Spatial Scale in Cellular Automata Markov Chain Simulation of Land Use Change." *International Journal of Geographical Information Science* 33, no. 5: 1040–1061.

Yang, J., W. Tang, J. Gong, R. Shi, M. Zheng, and Y. Dai. 2023. "Simulating Urban Expansion Using Cellular Automata Model With Spatiotemporally Explicit Representation of Urban Demand." *Landscape and Urban Planning* 231: 104640. https://doi.org/10.1016/j.landurbplan.2022.104640.

Yang, X. J. 2013. "China's Rapid Urbanization." *Science* 342, no. 6156: 310. https://doi.org/10.1126/science.342.6156.310-a.

Yao, Y., H. Zhang, Z. Sun, et al. 2023. "Fine-Grained Regional Economic Forecasting for a Megacity Using Vector-Based Cellular Automata." *International Journal of Applied Earth Observation and Geoinformation* 125: 103602. https://doi.org/10.1016/j.jag.2023.103602.

Yeh, A. G. O., and X. Li. 2006. "Errors and Uncertainties in Urban Cellular Automata." *Computers, Environment and Urban Systems* 30, no. 1: 10–28.

Yeh, A. G.-O., and X. Li. 2002. "A Cellular Automata Model to Simulate Development Density for Urban Planning." *Environment and Planning B: Planning and Design* 29, no. 3: 431–450. https://doi.org/10.1068/b1288.

Yoon, J. 2021. "Forecasting of Real GDP Growth Using Machine Learning Models: Gradient Boosting and Random Forest Approach." *Computational Economics* 57, no. 1: 247–265.

Yuan, W., Y. Cai, and J. Li. 2024. "Hybrid Network-Based Automatic Seamline Detection for Orthophoto Mosaicking." *IEEE Transactions on Geoscience and Remote Sensing* 62: 1–14.

Yuan, W., X. Yuan, Y. Cai, and R. Shibasaki. 2023. "Fully Automatic DOM Generation Method Based on Optical Flow Field Dense Image Matching." *Geo-spatial Information Science* 26, no. 2: 242–256.

Zeng, C., Y. Yao, J. Liu, et al. 2025. "CoCA: Spatial Cooperative Simulation and Future Prediction of "Land-Population-Economy" in Urban Agglomerations." *Landscape and Urban Planning* 263: 105442. https://doi.org/10.1016/j.landurbplan.2025.105442.

Zhang, B., S. Hu, H. Wang, and H. Zeng. 2023. "A Size-Adaptive Strategy to Characterize Spatially Heterogeneous Neighborhood Effects in Cellular Automata Simulation of Urban Growth." *Landscape and Urban Planning* 229: 104604. https://doi.org/10.1016/j.landurbplan.2022.104604.

Zhou, X., B. Wu, Y. Liu, Q. Zhou, and W. Cheng. 2023. "Synergistic Effects of Heat and Carbon on Sustainable Urban Development: Case Study of the Wuhan Urban Agglomeration." *Journal of Cleaner Production* 425: 138971.

Supporting Information

Additional supporting information can be found online in the Supporting Information section. **Table S1:** Robustness and computational performance of the developed DCA software. **Table S2:** Experimental settings for parameter sensitivity analysis. **Table S3:** Parameter sensitivity analysis for the neighborhood size. **Table S4:** Parameter sensitivity analysis for the cell radius. **Table S5:** Parameter sensitivity analysis for the number of decision trees. **Table S6:** Parameter sensitivity analysis for the sampling rate. **Table S7:** Parameter sensitivity analysis for the β in the RA term. **Table S8:** Accuracy comparison between the GDP simulations from 2010 to 2020 and 2000 to 2010 using different CA models.